Volume 1 | Number 1 | Jan 2013 | Pages 1–100

ChemComm

Chemical Communications
www.rsc.org/chemcomm

ROYAL SOCIETY OF CHEMISTRY

ROYAL SOCIETY OF CHEMISTRY

www.rsc.org/chemcomm

Journal Name

Chemical controls on uranyl citrate speciation and the self-assembly of nanoscale macrocycles and sandwich complexes in aqueous solutions.

M. Basile, D. K. Unruh, K. Gojdas, E. Flores, L. Streicher, and T.Z. Forbes[a]

Uranyl citrate forms trimeric species at pH>5.5, but exact structural characteristics of these important oligomers have not previously been reported. Crystallization and structural characterization of the trimers suggests the self-assembly of the 3:3 and 3:2 U:Cit complexes into larger sandwich and macrocyclic molecules. Raman spectroscopy and ESI-MS have been utilized to investigate the relative abundance of these species in solution under varying pH and citrate concentrations. Additional dynamic light scattering experiments indicate that self-assembly of the larger molecules does occur in aqueous solution.

The uranyl $(U(VI)O_2)^{2+}$ cation readily binds to a wide array of carboxylate ligands, but complexation with the citrate molecule $(H_4Cit = C_6H_8O_7)$ has broad reaching impacts on the environmental transport of radionuclides, remediation strategies, chelation therapies, and the development of novel materials. Complexation of the uranyl cation by citrate in environmental systems results in higher solubility, increased mobility in surface and subsurface waters, and enhanced availability for microbial and phytocoenosis communities.[1-4] Environmental restoration and phytoremediation strategies have been developed and implemented based upon the higher solubility of these uranyl species, where the addition of citrate can enhance plant uptake by over a 1000-fold or photodegrade readily under UV light.[1, 5] Furthermore, citrate has been identified as a chelation therapy for human patients with acute exposures to U due to the stability and mobility of the molecular citrate complexes in biological systems.[6] Strong bonding between the multidentate citrate ligand and the metal centre has also led to its use as an organic linker for the development of hybrid uranyl materials.[7-10]

While the importance of uranyl citrate complexation can be documented across a broad range of disciplines, the basic chemistry and aqueous speciation of this system is poorly understood. There is general agreement regarding the formation of a monomeric $UO_2(HCit)H^{n-1}$ (n = 0,1,2,3) species and the existence of a $(UO_2)_2(HCit)_2(OH)_n^{-(n+2)}$ (n = 0,1,2) dimer at pH<6.[11] The dimeric species $(UO_2)_2(HCit)_2^{2-}$ is the most dominant species in solution in this region and has a stability constant of 19.50 +/- 0.01.[11, 12] Structural information regarding the uranyl citrate dimer has been provided by crystallization from hydrothermal systems and EXAFS studies on aqueous solutions.[7, 13] At near neutral regions, trimeric or hexameric species have been proposed, but interpretations of the spectroscopic and potentiometric data vary widely.[11, 12, 14] The general interpretation is that there are two species that exist between a pH of 5-9 with $(UO_2)^{2+}:Cit$ ratios of 3:3 and 3:2, but the exact nature of these species has yet to be determined. Given the importance of the near neutral pH region to environmental and biological systems, it is critical to have a clear structural and spectroscopic understanding of these trimeric uranyl citrate species. In the current study, the synthesis, crystallization, and spectroscopic characterization of the 2:2 dimer $(UO_2)_2(HCit)_2^{2-}$ (**U2**), 3:3 trimer $(UO_2)_3O(Cit)_3^{5-}$ (**U3**), and an unexpected macrocyclic 3:2 species $[(UO_2)_9(OH)_3O_3(Cit)_6]^{15-}$ (**U9**) are described and characterized to clarify speciation in aqueous solutions.

A dimeric species is observed in **U2** and contains two uranyl pentagonal bipyramids with each *HCit* molecule located on opposite sides of the uranyl dimer. Chelation to the metal centres occurs through a shared deprotonated α-hydroxyl bridge and two deprotonated carboxylates functional groups. One arm of the citrate ligand remains protonated and uncomplexed to the uranyl cation, forming the $(UO_2)_2(HCit)_2^{2-}$ molecular unit. Crystallization of the dimeric species takes place through H-bonding interactions between the *HCit* ligand and the charge balancing organic bases (*pip, pyr, en*). The **U2** compound was formed under ambient conditions, but the dimer has also been isolated in high-temperature reactions by Thuery.[7] A previously reported EXAFS study also suggested formation of the dimer in aqueous solutions with reported U-U distances of 3.93 Å, which agrees well with the distances obtained by structural characterization (3.89 – 3.91 Å).[12] X-ray diffraction data also provides additional information regarding the absolute configuration of the ligand for **U2** with the free arm of the citrate molecule occurring in a transoid configuration in all solid state compounds.

The 3:3 and the 3:2 trimers crystallize in the **U3** and **U9** compounds, respectively (Fig. 1a and Fig. 1b). In both molecular components, the uranyl cation is surrounded by five equatorial ligands to create a pentagonal bipyramidal coordination geometry with an average equatorial U-O bond distance of 2.348(3) and 2.327(3) Å, respectively. Each trimeric species contains a central μ_3-O atom shared between three uranyl polyhedra with the *Cit* ligands bond to the edges of the trimer in a fashion similar to that of the dimeric species, i.e. shared deprotonated α-hydroxyl bridge and two deprotonated carboxylate functional groups. The 3:3 complex is fully chelated, but the 3:2 species contains a μ_2-OH group on one edge that serves as a bridging unit. In both cases, the carboxylate functional groups are deprotonated (as confirmed by IR spectroscopy) and the absolute configuration of the ligands result in an overall cisoid configuration for the free carboxylate arm.
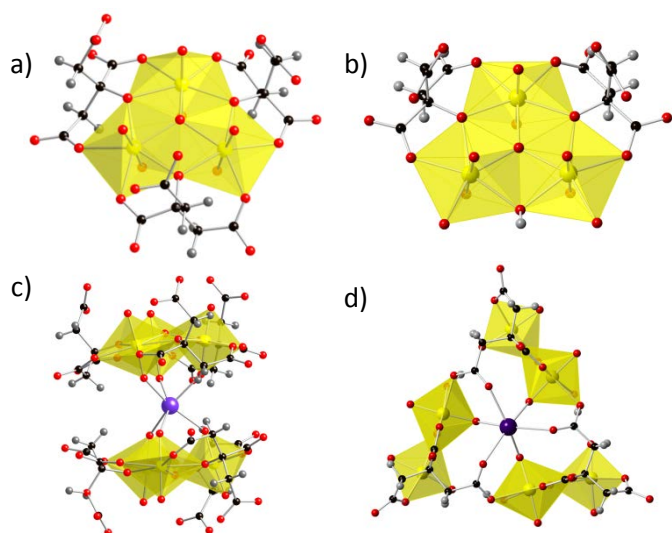
Figure 1. Molecular species isolated from uranyl citrate solutions: a) the 3:3 trimer (**U3**); b) the 3:2 trimer (**U9**); c) 6:6 sandwich complex (**U3**) and d) the 9:6 uranyl citrate macrocycle (**U9**). The UO_2 polyhedra are shown in yellow and the Na, O, C, and H atoms are represented by purple, red, black, and grey spheres, respectively.

Crystallization of solid phase also provides information regarding possible interactions between the molecular units. The **U3** trimeric species interacts with a Na^+ cation in the solid state structure to form a sandwich complex with a U:*Cit* ratio of 6:6 (Fig. 1c). The Na^+ cation in this case sits directly between the μ_3-O atom on each trimer and bonds to the six uranyl oxo atoms at an average distance of 2.352(3) Å. Self-assembly of a large molecular unit also occurs in **U9**, but forms a nanoscale macrocycle (Fig. 1d). The uncomplexed edge of the 3:2 trimer provides an ideal binding site for the deprotonated O atoms of the carboxylate on the neighbouring *Cit* ligand and the *cis*-confirmation, combined with the overall stereochemistry of the ligand provides the needed curvature. Overall, the molecular formula within **U9** is $[(UO_2)_9(OH)_3O_3(C_6H_4O_7)_6]^{15-}$ with additional Na^+ cations observed on the interior of the macrocycle, stabilizing the highly charged molecular species in solution.

Self-assembly of larger oligomers is quite prevalent for metal cations that readily undergo hydrolysis and nanoscale clusters have previously been reported for U(IV).[15, 16] The uranyl cation does not hydrolyze as readily, and often forms extended sheet topologies due to the anisotropic nature of the bonding.[15] Identity of the ligand in the equatorial plane is the largest driver of self-assembly and provides important control over the extent of curvature.[17] The most notable system that demonstrates this principle is the uranyl peroxide nanoclusters, in which the peroxide molecule influences the curvature, leading to a multitude of fullerene and cage topologies.[18, 19] Organic ligands have also been utilized to provide this type of self-assembly forming large cage cluster, such as the those created through linkages with calix[4,5]arene.[20] Solid state characterization of the 3:3 and 3:2 trimers also suggests that there could be additional self-assembly in solution, but we turn to additional spectroscopic and scattering tools to address this issue.

Raman spectroscopy is an excellent technique to investigate U(VI) speciation, given the strong stretching mode associated with the uranyl, and has been utilized previously to investigate uranyl citrate speciation.[21] The U=O symmetric stretching band (ν_1) is generally observed at 870 cm^{-1} for the pentaaqua uranyl complex and the peak will red shift 30-60 cm^{-1} depending on the complexing ligand and the degree of oligomerization. Solid state Raman spectroscopy was used to provide a basis for studies on the aqueous solution. In **U2**, the uranyl stretching band was located at 825 cm^{-1} with a red shift to 800 and 790 cm^{-1} observed for the 3:3 (**U3**) and the 3:2 (**U9**) trimers, respectively. A secondary peak located at approximately 814 cm^{-1} was also observed in all three spectra and was assigned to a C-O stretch of the complexed *Cit* molecule. Definitive assignment of vibrational bands in the solid state is important because it can be difficult to assign peaks in the related aqueous solutions, where several species can exist simultaneously. For example, Pasilis and Pemberton utilized Raman spectroscopy to provide information on the uranyl citrate speciation in aqueous solutions and assigned the band for the dimeric species at 826 cm^{-1}, but the 3:2 species was postulated to occur at 812 cm^{-1}.[21] Based upon our solid state analysis, the 812 cm^{-1} was likely associated with the citrate molecule and the third observed band at 795 cm^{-1} represented a trimeric species.

Solution based Raman spectroscopy experiments have been performed with U:*Cit* ratios of 1:1 and 1:2 ([0.5 mmol $(UO_2)(NO_3)_2$: 0.5mmol or 1.0mmol *Cit*], pH adjusted with 1M NaOH) with peak fitting utilizing the nitrate band at 1047 cm^{-1} to normalize the spectra. At a pH 3, the dimeric peak is dominant as seen by the large band at 826 cm^{-1}. With increasing pH, the band associated with the dimer decreases and peaks at 793 and 797 cm^{-1} are observed. Fitting the Raman bands for the two trimeric species presented some difficulties due to the high degree of overlap and broadness of the peaks. The peak at 812 cm^{-1} was also analysed (see supplemental information for additional details), providing information on the relative ratio of U:*Cit*. For the 1:1 solution, the band at 793 cm^{-1} suggests the presence of the 3:2 species and is confirmed by the U:*Cit* ratio. The band at 797 cm^{-1} in the 1:2 solution suggests the 3:3 species is favoured, but the intensities of the peaks suggest a 2:1 U:*Cit* ratio. As the peak at 814 cm^{-1} only occurs upon complexation of *Cit* by the metal, the observed deviation from the expected value could be due to changes in the Raman cross-section or presence of other species in solution, but additional investigations are necessary to confirm these hypotheses.

Given the inherent difficulties in distinguishing between the two trimeric species using spectroscopy, ESI-MS was utilized to try to provide additional evidence on the exact trimer present in buffered solutions. In the initial studies, solid state crystals were dissolved in aqueous solutions buffered with NH_4OH. Both the dimer [$2UO_2$–$2Cit$]$^{2-}$ at m/z = 459 and the 3:3 trimer [$3UO_2$–O–$3Cit + 6H$]$^{2-}$ at m/z = 698 were present upon dissolution of the solid material, but two fragments were found for **U9** [$3UO_2$–O–OH–$2Cit$–$3H$]$^{2-}$ at m/z = 610 and [$3UO_2$–O–OH–$2Cit + 2Na$]$^{3-}$ at m/z = 422. Similar ESI-MS experiments were performed on the 1:1 and 1:2 aqueous solution, but only pH 3 provided a simple fragmentation of the molecular species where a [UO_2-$2OH$-$3HCit$-$5H^+$-$2NH_4$]$^{2-}$ monomer at m/z = 456 dominated the spectrum. This fragmentation is more apparent with the higher pH solutions, which contained monomers, dimers, and trimeric forms with only the 3:3 trimer being observed under these conditions. The inability to observe the 3:2 species in solution is surprising, but could be due to increased fragmentation, or the lack of Na^+ in solution. Initially, the solutions used in the ESI-MS experiments were prepared using NaOH, but the formation of Na clusters in the spectra prevented accurate data analysis.

Formation of the uranyl citrate species in aqueous solutions has also been previously investigated by potentiometric techniques and NMR spectroscopy. Berto et al., observed the 2:2 dimer dominates when the pH was between 2.5 and 5 under a wide range of ionic strengths.[11] In all studies, including the current one, the 2:2 dimer is observed under acidic conditions. Berto et al. also found that a 3:2 trimeric species was the dominate species after a pH 6, and the 3:3 trimer was not considered a major species when the pH>6.[11] This is

in agreement with the ^{13}C NMR data collected by Nunes et al., which found that the 3:2 species was the dominant species under alkaline conditions.[12] The 3:3 complex may have also been observed in the NMR spectra from pH 5.5 to 8, but is absent at pH values higher than 8, Based upon these previous studies and our current work, the data suggests that the 3:2 and 3:3 trimers can both exist in solution simultaneously and that the equilibrium between the two species can be controlled by pH and ligand concentration.
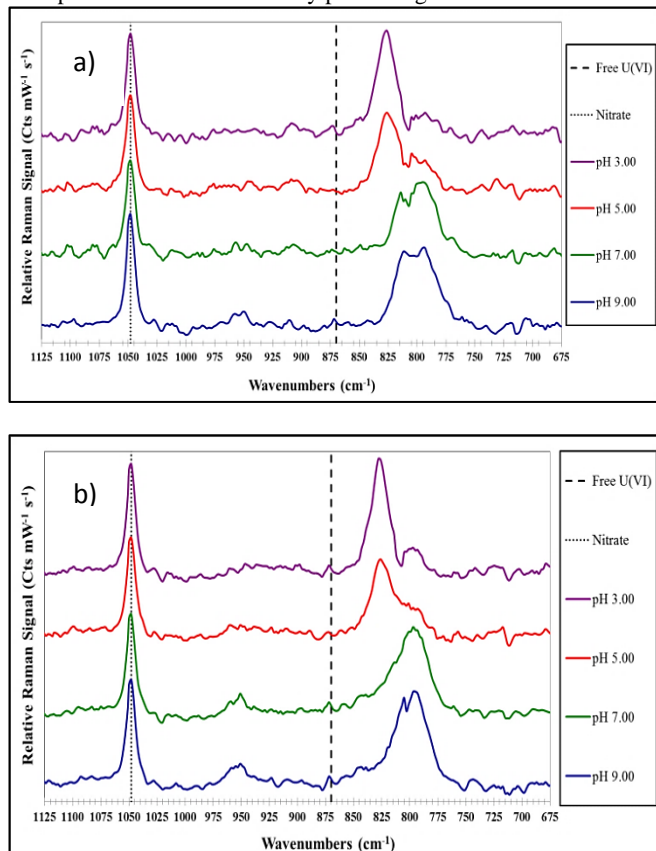

Figure 2. Raman spectra of aqueous solutions containing a) 1:1 and b) 1:2 U:*Cit* indicates a shift from a dominant dimeric species to a trimer with increasing pH. Peaks were normalized based upon the NO_3^- peak at 1047 cm^{-1} and the dashed line indicates the expected location of the ν_1 associated with the $[(UO_2)(H_2O)_5]^{2+}$ species.

Missing from the spectroscopic and ESI-MS studies is the evidence of the larger, self-assembled macrocyclic and sandwich complexes, which cannot be observed based upon these techniques. Formation of the 3:2 macrocyclic unit was previously suggested by the ^{13}C and ^{1}H NMR data because the signal for the ligand was equivalent, all coordinating sites were involved with metal bonding, and the structure remained rigid, as demonstrated by no change in the spectra from 275-320 K.[12] NMR data provides the relative ratios of the constituent as 3:2, but this ratio is maintained when the 9:6 macrocycle is formed. To provide additional evidence of the self-assembly of the trimeric species, dynamic light scattering studies were performed on the solutions with U:*Cit* concentrations of 0.2 M, resulting in an average hydrodynamic diameter of 1.76 nm observed in solution. Structural characterization of the **U9** 9:6 macrocycle provides an overall diameter of 1.36 nm based upon diametrically opposed points on the molecular unit and a slightly larger hydrodynamic diameter would be expected for this cluster based upon additional interactions with the Na^+ cations and first-shell H_2O molecules. A similar radius could be observed for the 3:3 sandwich complex, but is reliant on interactions with one Na^+ cation. This bonding will be weaker than those observed for the macrocycle resulting in limited stability and likely only to exist with high Na^+ concentrations. From the DLS experiments, we propose that the 9:6 macrocycle can exist in solution from the self-assembly of 3:2 trimeric building units.

Conclusions

Crystallization and structural characterization of uranyl citrate molecules provides crucial information regarding the dominant species that exist in aqueous systems and provides a strong foundation to explore these systems further with spectroscopic and scattering techniques. Providing absolute configurations and coordination modes of these species will lead to a deeper understanding of metal-ligand complexes, while providing essential information to studies investigating enhanced mobility in the environment and uptake by biological systems. Additional studies are necessary to provide a more robust understanding of the solution phase equilibrium between the two trimeric species, but the formation and self-assembly of these large, soluble oligomers has far reaching impacts on the complete picture of uranyl citrate speciation.

Notes and references

[a] University of Iowa, Department of Chemistry, Iowa City, IA 52242.
Electronic Supplementary Information (ESI) available: [synthesis, single-crystal XRD, FT-IR, TGA, ESI-MS, Raman]. CIF files available CCDC 1031409-1031413 See DOI: 10.1039/c000000x/

1. C. J. Dodge and A. J. Francis, *Environ. Sci. Technol.*, 1994, **28**, 1300-1306.
2. A. J. Francis and C. J. Dodge, *Environ. Sci. Technol.*, 1998, **32**, 3993-3998.
3. A. J. Francis, C. J. Dodge and J.B. Gillow, *Nature*, 1992, **356**, 140-142.
4. B. Huta, J. J. Lensboeur, A. J. Lowe, J. Zubieta and R. P. Doyle, *Inorg. Chim. Acta*, 2012, **393**, 125-134.
5. J. W. W. Huang, M. J. Blaylock, Y. Kapulnik and B. D. Ensley, *Environ. Sci. Technol.*, 1998, **32**, 2004-2008.
6. G. D. Lawrence, K. S. Patel and A. Nusbaum, *Pure Appl. Chem.*, 2014, **86**, 1105-1110.
7. P. Thuery, *Inorg. Chem.*, 2007, **46**, 2307-2315.
8. P. Thuery, *Chem. Comm.*, 2006, 853-855.
9. P. Thuery, *Crystengcomm*, 2008, **10**, 79-85.
10. J. Lhoste, N. Henry, P. Roussel, T. Loiseau and F. Abraham, *Dalton Trans.*, 2011, **40**, 2422.
11. S. Berto, F. Crea, P. G. Daniele, C. De Stefano, E. Prenesti and S. Sammartano, *Radiochim. Acta*, 2012, **100**, 13-28.
12. M. T. Nunes and V. M. S. Gil, *Inorg. Chem. Acta*, 1987, **129**, 283-287.
13. P. G. Allen, D. K. Shuh, J. J. Bucher, N. M. Edelstein, T. Reich, M. A. Denecke and H. Nitsche, *Inorg. Chem.*, 1996, **35**, 784-&.
14. I. Feldman, J. R. Havill and W. F. Neuman, *J. Am. Chem. Soc.*, 1954, **76**, 4726-4732.
15. K. E. Knope and L. Soderholm, *Chem. Rev.*, 2013, **113**, 944-994.
16. C. Falaise, C. Volkringer, J.-F. Vigier, A. Beaurain, P. Roussel, P. Rabu and T. Loiseau, *J. Am. Chem. Soc.*, 2013, **135**, 15678-15681.
17. M. B. Andrews and C. L. Cahill, *Chem. Rev.*, 2013, **113**, 1121-1136.
18. P. C. Burns, *Comptes Rendus Chimie*, 2010, **13**, 737-746.
19. P. C. Burns, K. A. Kubatko, G. Sigmon, B. J. Fryer, J. E. Gagnon, M. R. Antonio and L. Soderholm, *Angew. Chem.-Int.Ed.*, 2005, **44**, 2135-2139.
20. S. Pasquale, S. Sattin, E. C. Escudero-Adan, M. Martinez-Belmonte and J. de Mendoza, *Nature Comm.s*, 2012, **3**, 1-7.
21. S. P. Pasilis and J. E. Pemberton, *Inorg. Chem.*, 2003, **42**, 6793-6800.